

SPIRAL ARM AMPLITUDE VARIATIONS AND PATTERN SPEEDS IN THE GRAND DESIGN GALAXIES M51, M81, AND M100

BRUCE G. ELMEGREEN,¹ DEBRA MELOY ELMEGREEN,^{1,2} AND PHILIP E. SEIDEN¹

Received 1988 December 13; accepted 1989 January 20

ABSTRACT

The amplitudes of the spiral arms in M51, M81, and M100 have been found to oscillate smoothly around their mean radial variations with a characteristic wavelength of ~ 5 kpc and a relative amplitude of 100%. The phases of the spirals and the relative amplitudes of the $m = 4$ and $m = 2$ Fourier components oscillate slightly too. The absence of corresponding color variations and the symmetry of the amplitude peaks with respect to the galaxy centers suggest that the oscillations are an intrinsic part of the stellar spiral density wave. This observation confirms predictions of both the modal and stellar dynamical theories of spiral structure. The radial positions of the prominent gaps in the spiral arm amplitudes are compared to the expected positions of various wave resonances. Excellent fits are obtained for M81 and M100 if the gaps are at the 4:1 resonances; then the spirals end at the outer Lindblad resonances, the inner Lindblad resonances are well shielded, and the primary star formation ridges and dust lanes are between the 4:1 and corotation resonances. Prominent interarm features and spurs also occur at the 4:1 and corotation resonances in these galaxies. The situation is similar but more complicated in M51, which requires two spiral systems to cover the disk. The best fit is for an inner spiral mode that has an outer Lindblad resonance at the position of a prominent arm intensity gap, and an outer material spiral that corotates with the companion. Then the average position of the inner Lindblad resonances of the outer material arms occurs at the same radius as the corotation resonances of the inner mode. This conjunction of resonances may explain how the companion to M51 triggered a strong spiral throughout most of the disk.

Subject headings: galaxies: individual (M51, M81, M100) — galaxies: internal motions — galaxies: structure

I. INTRODUCTION

In the modal theory of galactic spiral structure (see Bertin *et al.* 1989), the amplitude of a prominent two-arm spiral pattern should oscillate slightly with galactocentric distance because of an interference between the outward and inward propagating waves (Lin 1983). In the stellar dynamical theory also (Contopoulos and Grosbøl 1986), the spiral arm amplitudes should oscillate because of differential crowding near and between wave-orbit resonances.

We have found two and three cycles of such oscillations in computer enhanced images at B and I passbands of the grand design galaxies M81 (NGC 3031) and M100 (NGC 4321), respectively, and we have found what is likely to be one cycle of such an amplitude variation in M51 (NGC 5194). These three galaxies are the most symmetric and global of the two-arm spiral galaxies in our near-infrared survey (Elmegreen 1981), so the occurrence of such spiral amplitude oscillations could be common among galaxies of this type. Similar variations in the brightnesses of spirals have also been observed in the grand design galaxy NGC 1376 (Grosbøl 1988). In § III, we use the positions of these features to suggest possible spiral arm pattern speeds.

II. OBSERVATIONS

Blue (B band) and near-infrared (I band) photographic plates of M81, M100, and M51 were obtained at the Palomar 1.2 m Schmidt telescope during 1979–80 as part of a broad observing program on the structure of galaxies. The plate-filter combinations were $B = \text{IIaO} + \text{GG13}$ and $I = \text{IV}$

$N + \text{Wr88A}$. Sensitometer wedges were applied shortly after each 10 m (B) or 90 m (I) exposure. The plates were scanned with the IBM microdensitometer (Angiello *et al.* 1985) and converted to relative intensity using piece-wise cubic fits to the sensitometer wedges; plate fog and sky brightness were subtracted in the usual way.

The resultant 512×512 image of each galaxy was stretched along the minor axis by a factor equal to the inverse of the cosine of the inclination (from de Vaucouleurs, de Vaucouleurs, and Corwin 1976). The result is an image that simulates the face-on orientation of the galaxy, with some distortion of three-dimensional components (e.g., the bulge and any warps). The average radial light profile in the disk of each galaxy was also subtracted from the image in order to emphasize the spiral arms and other nonaxisymmetric structures (e.g., star formation patches). The details of these procedures were given by Seiden, Elmegreen, and Elmegreen (1989).

The galaxy images were also replotted in polar coordinates, pixel by pixel, with the azimuthal angle along the abscissa and the logarithm of the radius along the ordinate. Interpolation and averaging between neighboring pixels was necessary. Such $\log R - \theta$ diagrams straighten out logarithmic spiral arms, and they illustrate the global patterns and symmetries much better than conventional images (see also Iye *et al.* 1982).

Figures 1–3 (Plates 17–19) show the B band (*top*) and I band images of M81, M100, and M51, rectified to face-on orientations with the average radial light profiles subtracted. The calibration bar on the left in the rectified images represents 100 pixels. The length of the bar on the right represents the isophotal radius, $R_{2.5}$, obtained from $D_{2.5}$ in de Vaucouleurs, de Vaucouleurs, and Corwin (1976); the tic mark on this bar indicates the center of the galaxy. Figure 4 (Plate 20) shows the $\log R - \theta$ plots of these galaxies in the B band.

¹ IBM Research Division, T. J. Watson Research Center, Yorktown Heights, NY.

² Vassar College Observatory.

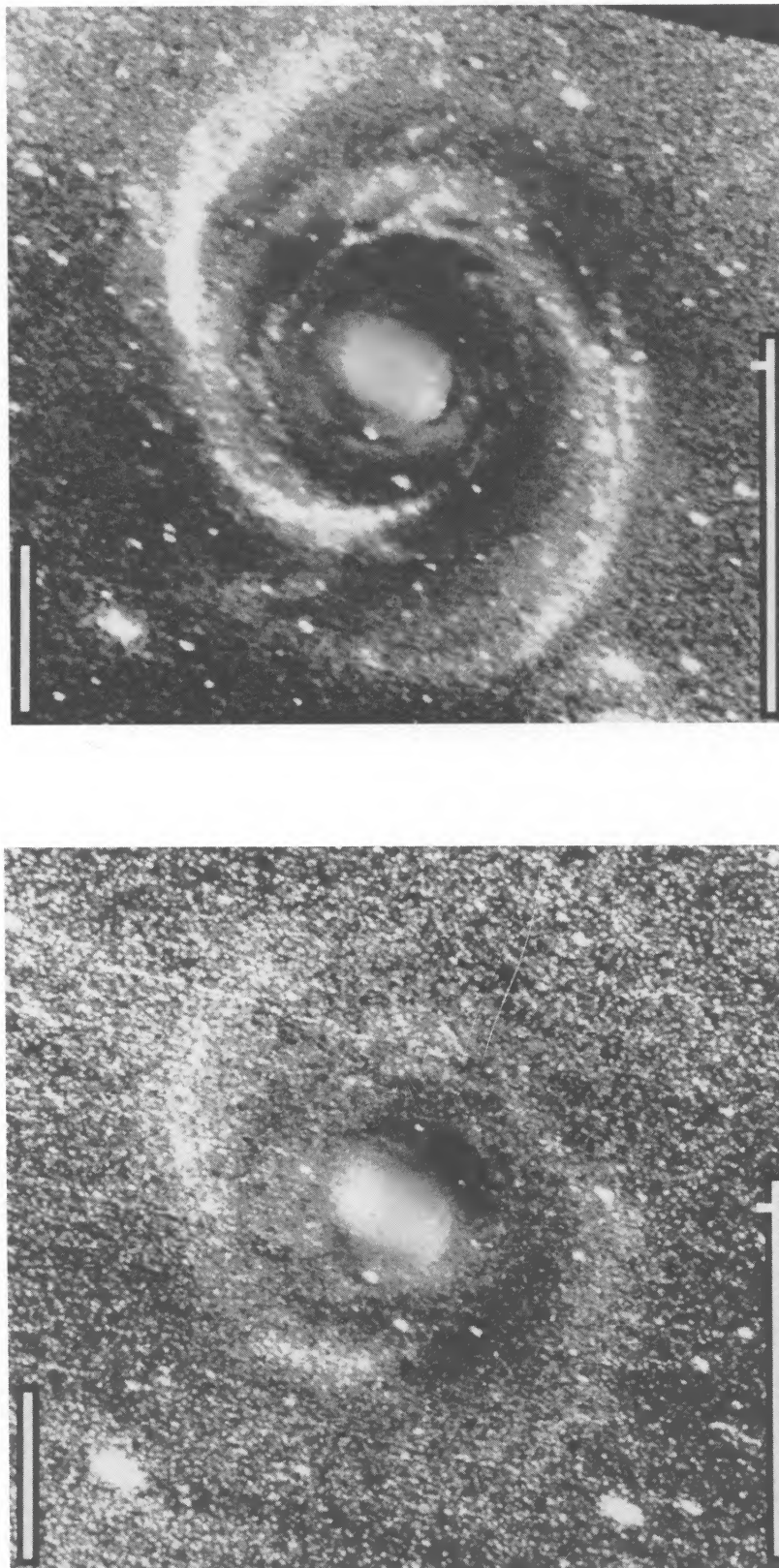


FIG. 1.—Blue image (*top*) and near-infrared image (*bottom*) of M81 rectified to a face-on orientation, with the average radial light profile subtracted, and with the rms fluctuations in the nonaxisymmetric residual normalized to a constant value for all radii. The calibration bar on the left is 100 pixels, and the bar on the right is R_{25} , with a tic mark indicating the position of the galaxy center.

ELMEGREEN *et al.* (see 343, 602)

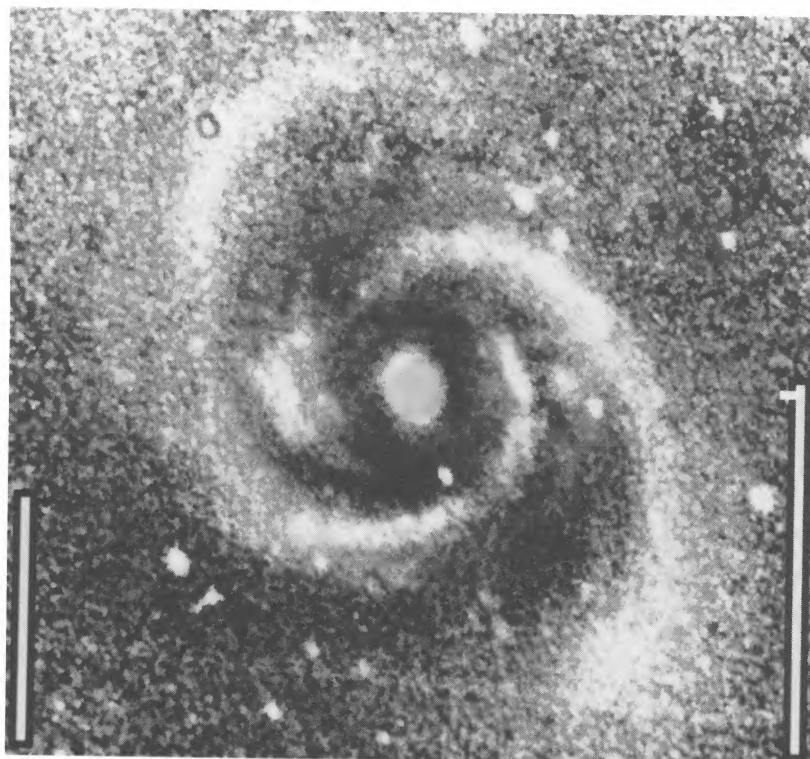
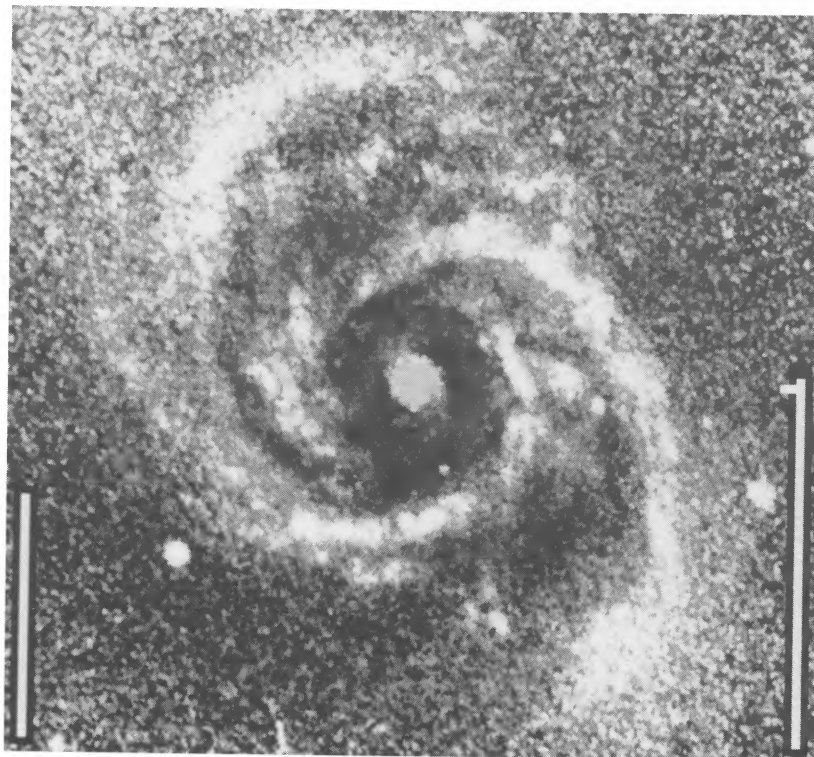


FIG. 2.—Blue (*top*) and near-infrared images of M100, enhanced as in Fig. 1

ELMEGREEN *et al.* (see 343, 602)

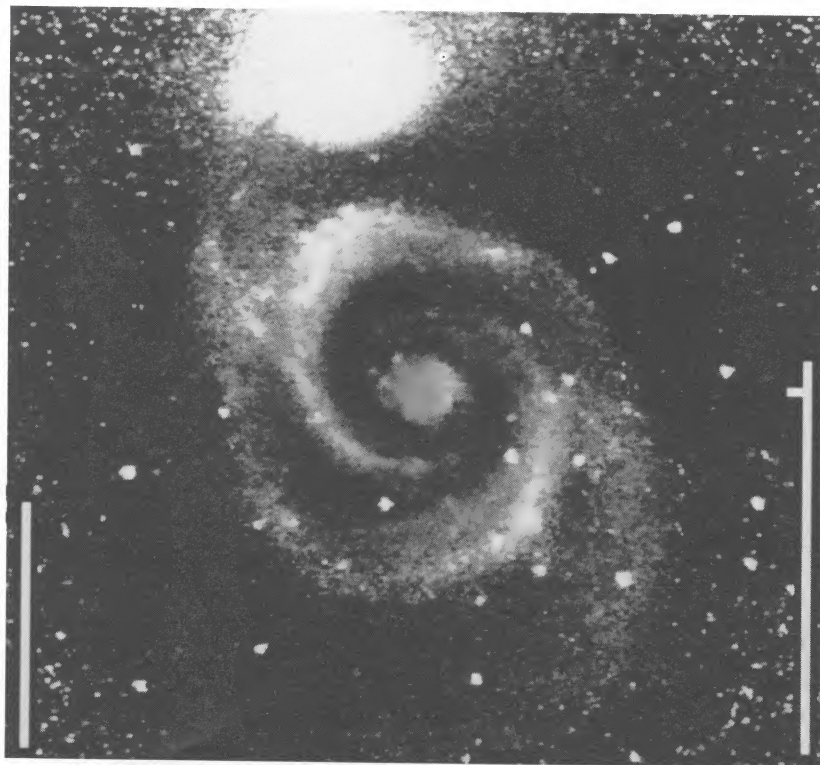
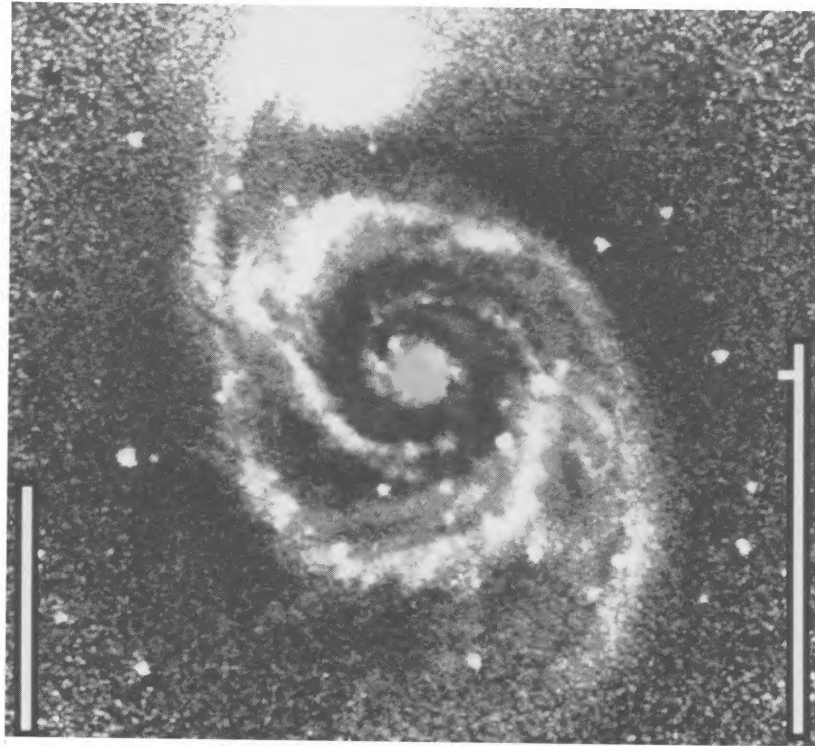


FIG. 3.—Blue (*top*) and near-infrared images of M51, enhanced as in Fig. 1

ELMEGREEN *et al.* (see 343, 602)

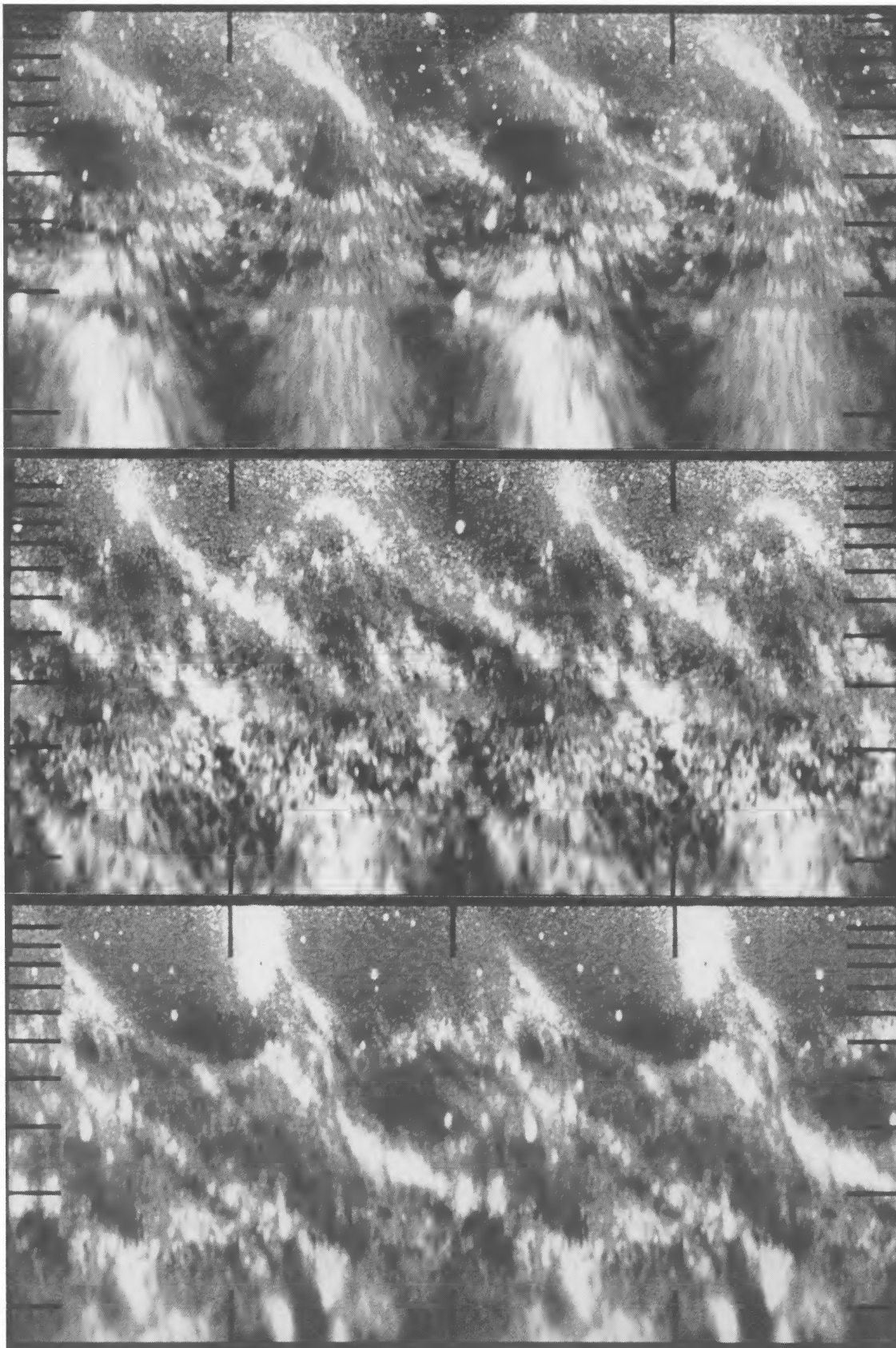


FIG. 4.—Three galaxies in blue light, M81 (*top*), M100 (*middle*), and M51 (*bottom*) are plotted in $\log R - \theta$ coordinates. The vertical axis is $\log R$, and the tic marks are in units of $0.1 R_{25}$. The horizontal axis is the azimuthal angle, measured counterclockwise from the eastern major axis; the tic marks are in units of 180° , so two full cycles are shown.

ELMEGREEN *et al.* (see 343, 602)

1989ApJ...343..602E

In Figure 1, the amplitude of each spiral arm in M81 can be seen to have two prominent maxima. For the eastern arm, these maxima occur at radii (in units of R_{25}) and azimuthal angles (measured counterclockwise from the vertical) equal to (0.43, 160°) and (0.75, 40°). The western arm has exactly symmetric versions of these maxima. In Figure 2, the spiral arms of M100 have three maxima each, at (0.27, 280°), (0.50, 140°) and (0.90, 40°) for one arm and at symmetric positions for the other arm. In Figure 3, the spiral arms of M51 have single prominent maxima, at (0.4, 30°) and at the symmetric position across the center. These maxima are evident in both the rectified images and in the $\log R - \theta$ plots.

The spacings of the spiral arm maxima in M100 are approximately logarithmic, as expected for intersection points of leading and trailing logarithmic spirals of comparable wavelength. This agrees with predictions of the modal theory by Bertin *et al.* (1989) and Lin (private communication). The angles between the peaks were also predicted by Lin (private communication) to be $\sim 90^\circ$ or larger. In M81, they are $\sim 120^\circ$, and in M100 they are $\sim 100^\circ$ and $\sim 140^\circ$.

The shapes of the main spiral arms in these three galaxies are not simple mathematical functions (e.g., see also Kennicutt 1981). If we fit straight lines through the arms in Figure 4 (thereby assuming logarithmic spirals), the pitch angles are derived to be $\sim 16^\circ$, 18° , and 15° , for M81, M100, and M51, respectively, with a $\pm 4^\circ$ variation from segment to segment.

To determine the amplitude and degree of symmetry of these spiral arm variations, azimuthal intensity profiles were

made from the original *B* and *I* band images at inclination-corrected radii spaced by $0.025R_{25}$, and the arm and interarm peaks at each radius were measured. The intensities of the arms were then divided by the average intensities of the adjacent interarm regions to get the arm/interarm intensity contrast at each radius. The result, converted into magnitudes [$= 2.5 \log_{10}(I_{\text{arm}}/I_{\text{interarm}})$], is shown in Figure 5. The two lines in each plot are for the two main spiral arms. Figure 5 indicates that the amplitude variations are present in both the *B* and *I* bands, with approximately the same relative amplitudes, and that the peaks occur at approximately the same radii and with the same amplitude for each arm. The large feature in the outer part of M51 is the companion galaxy, NGC 5195, which is more prominent in the *I* band.

Fourier components for the uncorrected azimuthal profiles in the *B* and *I* bands were also determined as a function of radius. In Figure 6, a solid line plots one-half of the peak to peak amplitude of the bisymmetric part of the spiral arms, divided by the average amplitude of the arms, which is all derived from the ratio $(F_2 + F_6)/(F_0 + F_4 + F_8)$ for Fourier components F_i . The plotted points (*right-hand axes*) are the phases of the $m = 2$ component; these phases are the angles at the peaks of the spiral arm crests, measured counterclockwise from the eastern major axis, in units of 360° . The oscillations in the spiral arm amplitudes that were present in Figure 5 are also present in Figure 6, which shows essentially the same result but uses a more objective method. Figure 6 also indicates that the phase of each spiral changes abruptly between amplitude

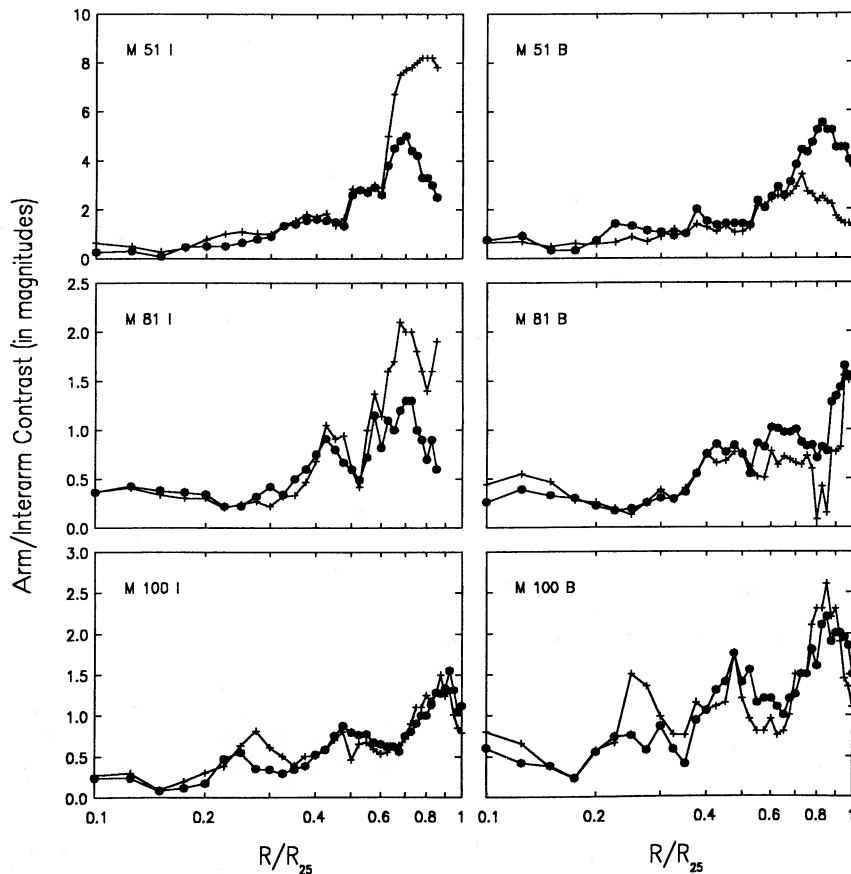


FIG. 5.—The magnitude differences between the arms and the interarms are plotted as a function of radius for each arm

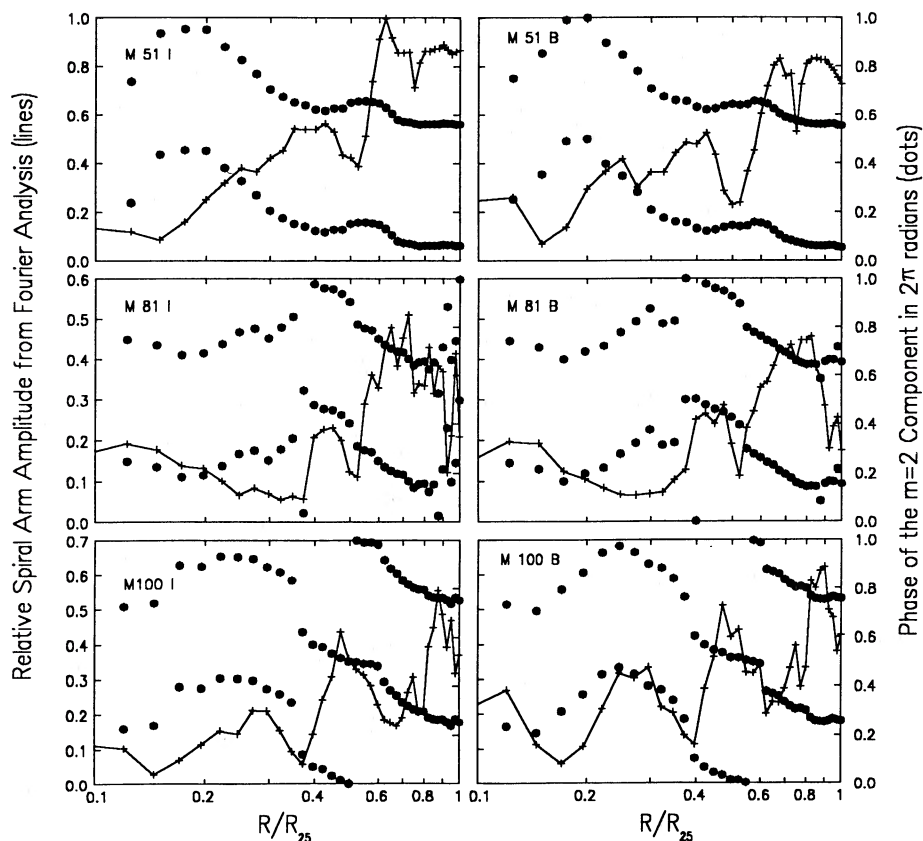


FIG. 6.—The spiral arm amplitudes determined from the even components of a Fourier decomposition (*left-hand axes, solid lines*) and the phases of the $m = 2$ component (*right-hand axes, dots*) are plotted as a function of radius. The amplitudes are defined to be one-half the peak values minus the mean values, divided by the mean values, or $(F_2 + F_6)/(F_0 + F_4 + F_8)$ for Fourier components F_i .

cycles. The gradient in the phase, which on these logarithmic radial plots is equal to the inverse of the tangent of the pitch angle, changes very slightly or not at all with each cycle.

The shape of the azimuthal profile through a spiral arm varies with the amplitude cycle too. Figure 7 plots again the relative amplitude of the even component, as in Figure 6, along with the ratio F_4/F_2 (*dashed lines, right-hand axes*). The ratios F_4/F_2 are anticorrelated with the spiral arm amplitude peaks in M81 and M100; i.e., this ratio becomes large at the radii where the spiral arm amplitudes are small. This variation in F_4/F_2 results from a variation in the prominence of interarm features, which tend to occur at the radii where the main spiral arms have a depression in intensity.

III. DISCUSSION

The amplitudes of the spiral arms in M51, M81, and M100 oscillate smoothly with radius. These oscillations are almost perfectly symmetric about the galaxy centers, and they are approximately equal in the blue and near-infrared passbands. This implies that the variations are probably not the result of star formation (e.g., “beads on a string”), but they are an intrinsic part of the stellar wave pattern. In the modal theory due to Lin and collaborators, they can be interpreted as evidence for oscillations of the radial eigenfunctions, as illustrated, for example, in Figures 12 and 13 of Bertin *et al.* (1989). In the stellar dynamical theory for non-linear spirals (Contopoulos and Grosbøl 1986, 1988), they are evidence for

stellar orbit crowding between resonances. Here we interpret this latter theory loosely, and expect only a minimum in the spiral arm amplitude at the 4:1 resonance, instead of an end to the spiral structure. Then some of the observed intensity minima can be placed at the 4:1 resonance, which is where $\Omega - \kappa/4$ equals the pattern speed. We base this interpretation on the occurrence of similar minima in the theoretical spiral arms in Figure 16 of Contopoulos and Grosbøl (1988). In what follows, the position of this resonance, and of the Lindblad and corotation resonances, are determined from our photographs and from published rotation curves and power law extrapolations to these rotation curves, i.e., $v(r) \propto R^\alpha$. The results are summarized in Figures 8–10 (Plates 21–23).

In M81, the rotation curve in Visser (1980) has approximately $\alpha = -0.20$ between $0.4R_{25}$ and R_{25} , so corotation should be at a radius equal to $1/0.73$ times the radius of the 4:1 resonance. If the minimum at $\sim 0.51R_{25}$, from Figures 5 or 6, is the 4:1 resonance, then corotation should be at $0.70R_{25}$, which is ~ 8.9 or 8.4 kpc from the center of the galaxy, for a distance of 3.25 Mpc and $R_{25} = 12.7 = 12.0$ kpc. Nothing obvious happens to the stellar spiral at this corotation point. The circular velocity at 8.4 kpc from the center is ~ 220 km s $^{-1}$ (Visser 1980), so the pattern speed is ~ 26 km s $^{-1}$ kpc $^{-1}$, which is larger than Visser's (1980) value of 18 km s $^{-1}$ kpc $^{-1}$. The outer Lindblad resonance occurs at 1.5 times the corotation radius for $\alpha = -0.2$, which is at $1.05R_{25}$ in this model, and close to the outer extent of the spiral in Figure 4. Figure 4 also indicates that the prominent spiral in M81 stops in the inner part at

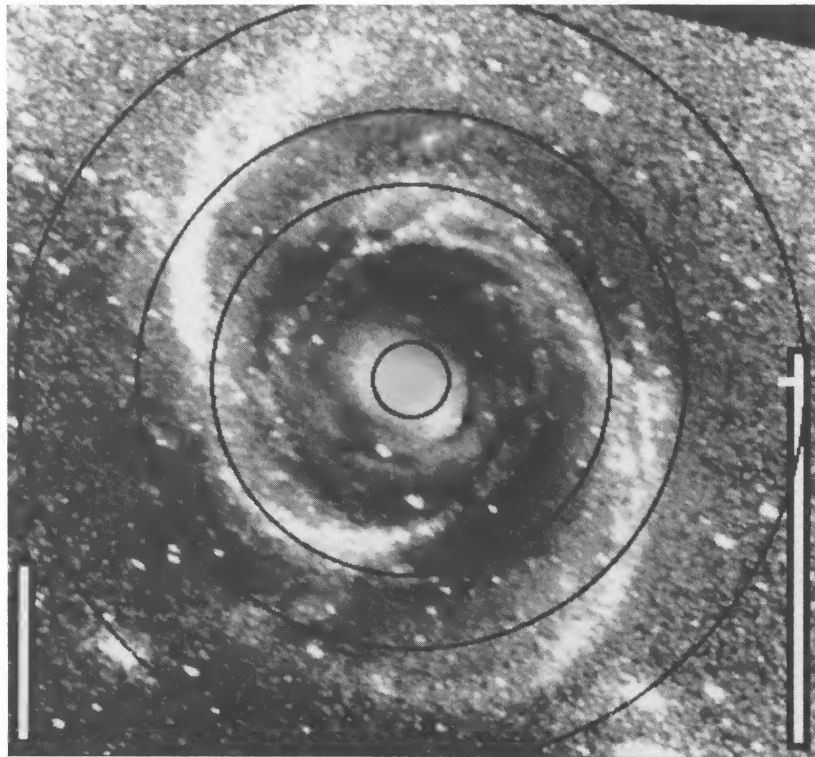


FIG. 8.—Rectified blue image of M81 with superposed radii of the four resonances, which, in order, are the inner Lindblad, 4:1, corotation, and outer Lindblad resonances

ELMEGREEN *et al.* (see 343, 604)

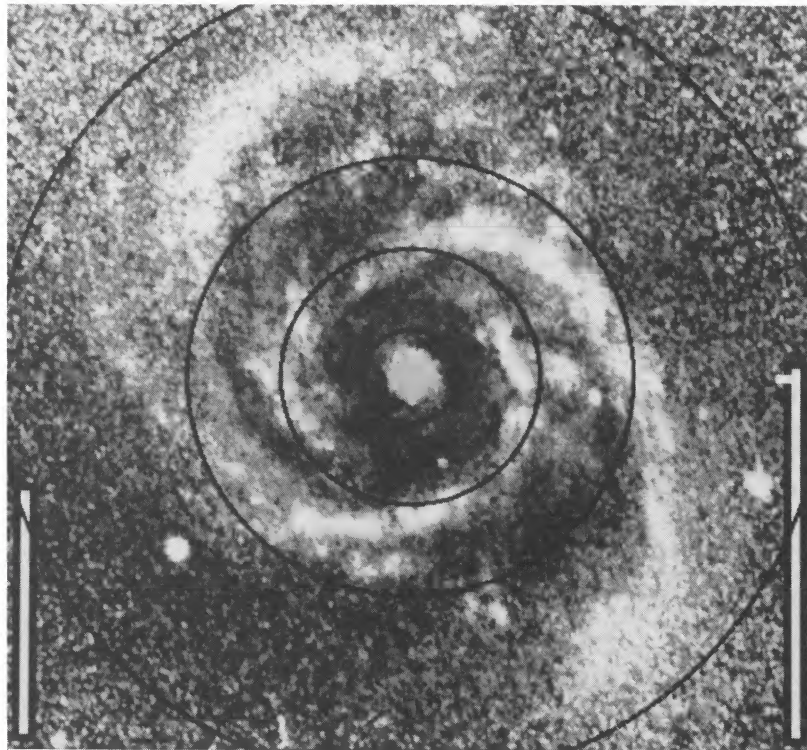


FIG. 9.—Rectified blue image of M100 with superposed radii of the four resonances, which, in order, are the inner Lindblad, 4:1, corotation, and outer Lindblad resonances

ELMEGREEN *et al.* (see 343, 604)

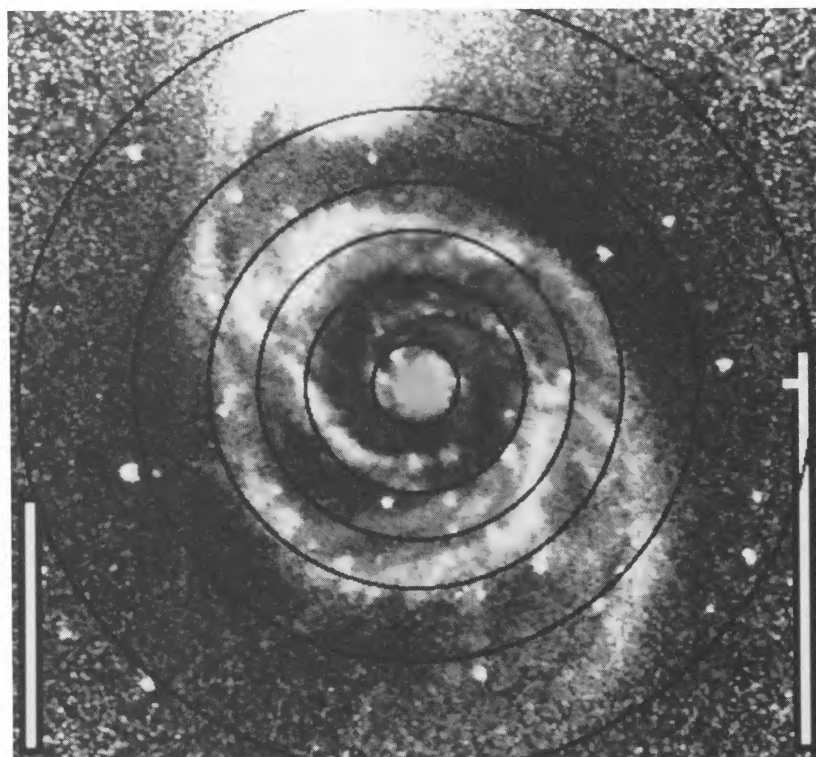


FIG. 10.—Rectified blue image of M51 with superposed radii of six resonances, which, in order, are the inner Lindblad, 4:1, corotation, and outer Lindblad resonance of the inner mode, and the 4:1 and corotation resonance of the outer spiral. The inner Lindblad resonance of the outer spiral is at the same radius as the corotation resonance of the inner spiral.

ELMEGREEN *et al.* (see 343, 604)

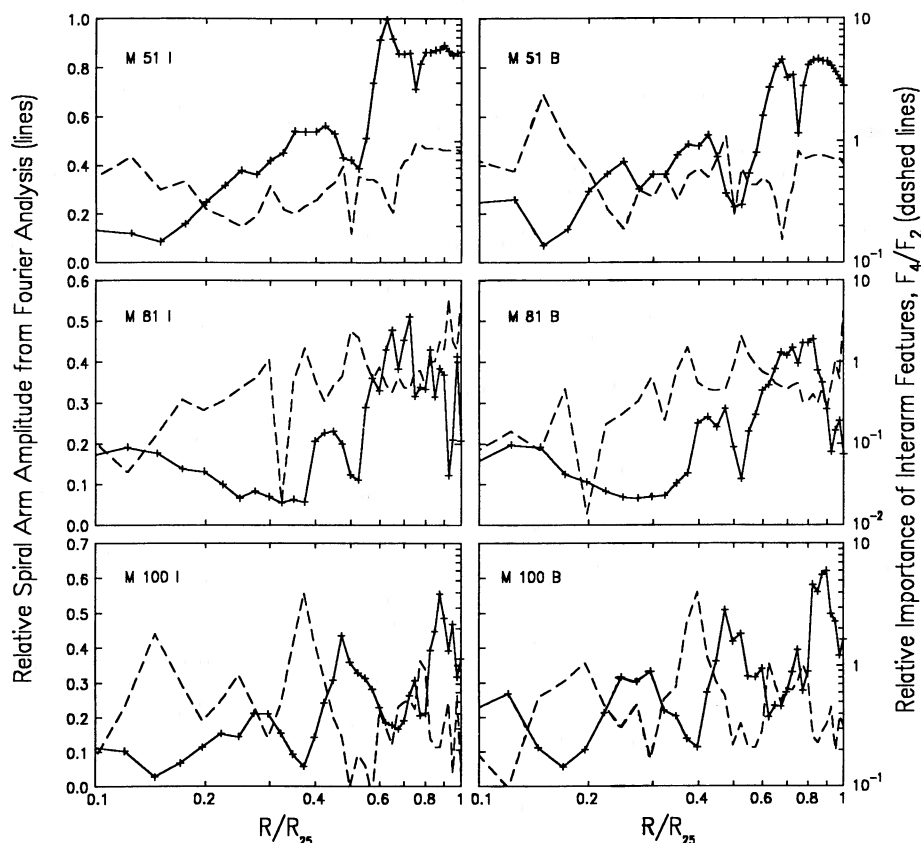


FIG. 7.—The spiral arm amplitudes from Fig. 6 are shown (solid lines, left-hand axes), along with the ratios of the $m = 4$ to the $m = 2$ Fourier components (dashed lines, right-hand axes), plotted as a function of radius. For M81 and M100, the ratio F_4/F_2 is anticorrelated with the amplitude of the arms.

$\sim 0.35R_{25}$. This is *outside* the inner Lindblad resonance, which is at ~ 1.2 kpc $\approx 0.10R_{25}$ according to Figure 3 in Visser (1980), with our pattern speed. Thus, in this model, the wave apparently avoids the inner Lindblad resonance by a wide margin; the inner extent of the arm presumably corresponds to a point of wave reflection (e.g., Lau, Lin, and Mark 1976). The arms extend from this inner reflection point at 4.2 kpc, to the outer Lindblad resonance at 12.6 kpc, with a prominent gap at the 4:1 resonance at 6.1 kpc and nothing obvious in the stellar component at the corotation resonance at 8.4 kpc. This is illustrated in Figure 8.

Note that there is a weak blue spiral feature between the inner Lindblad resonance and the reflection point in M81. This weak feature is also barely evident on the photograph in Sandage (1961), where it shows up as a dust spiral. Perhaps the wave penetrates the reflection point primarily in the gas. (The $m = 2$ Fourier component for the inner region of M81, shown in Fig. 6, is a result of the inclined bulge; the $m = 2$ phase is constant there, so the feature is radial, not spiral.)

Note also that in the region of the gap in M81, at $0.51R_{25}$, there is some interarm emission or a spiral arm spur in the north that has the effect of thickening the arm in conventional photographs, as in Sandage (1961). This emission is $\sim 90^\circ$ away from where the main arms cross the 4:1 radius (see Figs. 1, 4, and 8). This material gives the azimuthal profiles a substantial $m = 4$ component, which explains why the F_4/F_2 ratio increases at $0.51R_{25}$ in Figure 7. This position is filled with dust features on Figure 3c in Kaufman *et al.* (1989), and there is a similar jump in the displacement of matter from the spiral

arm minimum at this position in Figure 6 of Kaufman *et al.* (1989). We speculate that this interarm emission and dust is from star fluid compression and possibly gaseous shocks and star formation at orbital loops that are predicted to occur 90° from the main arms at approximately the radius of the 4:1 resonance (Shu, Milione, and Roberts 1973; see Fig. 10 in Contopoulos and Grosbøl 1986).

Another consideration for M81 is to take the outer extent of the arm, at $\sim 1R_{25}$, to be the 4:1 resonance, as suggested by Contopoulos and Grosbøl (1986). Then corotation is at ~ 16 kpc, the pattern speed is ~ 10 km s $^{-1}$ kpc $^{-1}$, and the inner Lindblad resonance is at ~ 9 kpc, which is outside the inner limit of the spiral by a factor of 2. This position for an inner Lindblad resonance is not possible if this resonance absorbs wave energy.

A similar analysis can be applied to M100, which has two gaps, at $0.35R_{25}$ and $0.65R_{25}$. The inner limit of the spiral is $\sim 0.2R_{25}$ and the outer limit is nearly $1.1R_{25}$ (see Figure 4). We use the rotation curve in Rubin, Ford, and Thonnard (1980), which gives $\alpha \approx 0.1$ between $0.2R_{25}$ and $0.65R_{25}$. We assume the distance is 20 Mpc (Rubin, Ford, and Thonnard 1980) and that $R_{25} = 3/42 = 19.9$ kpc. Suppose first that the inner gap, at $0.35R_{25}$, is the 4:1 resonance. Then corotation is at 1.67 times this radius, or $0.6R_{25}$, which is close to, but not exactly at, the next gap. The outer Lindblad resonance is at 1.85 times the corotation radius, or $1.1R_{25}$, which is the outer extent of the spiral. The inner Lindblad resonance is at 0.22 times the corotation radius, or $0.13R_{25}$, which is well inside the inner extent of the spiral. Thus a good fit to M100 places the spiral from an

inner reflection point at 4 kpc to the outer Lindblad resonance at 22 kpc, with a gap at the 4:1 resonance at 7.0 kpc and another gap close to corotation at 12 kpc. These radii are illustrated in Figure 9. As for M81, there is a faint gaseous spiral between the inner Lindblad resonance at 2.6 kpc and the main spiral wave reflection point at 4 kpc.

Note that the position for corotation in M100 is at the end of most of the bright star formation in the spiral arms (see Fig. 9 and Sandage 1961, p. 28); the spiral arms beyond this $0.65R_{25}$ gap barely show on the photograph in Sandage (1961) and the arms get relatively smooth in Figure 9. The gap could be the result of a local disorganization of the star formation pattern at the corotation radius. With corotation at $0.6R_{25}$, the pattern speed is $17 \text{ km s}^{-1} \text{ kpc}^{-1}$.

Both gaps in M100 correspond to the (only) positions of prominent interarm emission (Fig. 9). The proposed 4:1 resonance has a spur 90° away from where it intersects the arm (see also Sandage 1961), and the corotation resonance has much interarm star formation. This explains why the F_4/F_2 ratio increases at these radii (Fig. 7). The spur at the proposed 4:1 resonance could be the result of orbit crowding and gaseous shocks there, as in M81. The interarm emission at the proposed corotation resonance (the $0.65R_{25}$ gap) could be the result of star formation occurring independently of the wave, i.e., without the organization from a strong density wave shock. Local gravitational instabilities in the gas could initiate such star formation.

A different consideration for M100 is to place the 4:1 resonance at the $0.65R_{25}$ gap. Then corotation is at $1.1R_{25}$, which is the visible edge of the spiral (and well outside the apparent edge in the photograph in Sandage 1961). The inner Lindblad resonance in this case is approximately at $0.24R_{25}$, which is just at the inner boundary of the spiral, or possibly even slightly outside the inner boundary. The $0.35R_{25}$ gap has no significant in this interpretation. A fit with the 4:1 resonance at the outer extent of the spiral, at $1.1R_{25}$, places corotation at $1.8R_{25}$ and the inner Lindblad resonance at $0.4R_{25}$, which is close to the inner gap. The spiral has to extend inside this resonance, however, and that is unlikely. The best fit has the 4:1 resonance at the $0.35R_{25}$ gap, as discussed above.

In M51 there is a gap at $\sim 0.52R_{25}$, and the spiral extends from $\sim 0.1R_{25}$ to $1.0R_{25}$. We use the rotation curve in Tully (1974a), which gives $\alpha \approx -0.16$ from $25''$ to $300''$. Suppose first that the gap is at the 4:1 resonance. Then corotation is at $0.7R_{25}$, giving a pattern speed of $\sim 40 \text{ km s}^{-1} \text{ kpc}^{-1}$, and the inner Lindblad resonance is at $0.2R_{25}$, from Figure 5 in Tully (1974b). This inner resonance is outside the inner limit of the spiral, and so is unacceptable.

A better fit to M51 was suggested by Tully (1974b): corotation is at 2.5 kpc = $0.4R_{25}$ (for a galactic distance of 4 Mpc), the inner Lindblad resonance is at 0.6 kpc = $0.1R_{25}$, and the outer Lindblad resonance is at 3.35 kpc = $0.53R_{25}$. The pattern speed is $90 \text{ km s}^{-1} \text{ kpc}^{-1}$. In this model, the inner spiral wave ends at its outer Lindblad resonance, as in M81 and M100, and this termination is observed here as a local decrease in the spiral arm intensity, at $0.52R_{25}$. Figure 10 illustrates the positions of these resonances. The inner Lindblad resonance is where the arms turn into an oval pattern. The 4:1 resonance occurs where the inner arms begin to have spurs or a feather-like structure in all 4 directions, north, west, south, and east (these show up better in Sandage 1961, p. 26). These could be manifestations of the orbital loops discussed by Contopoulos and Grosbøl (1986). The corotation radius occurs

where the bright southern arm has a bifurcated dust lane, and the northern arm sharply bends to the west.

The strong spur in the west is at corotation too. The main star formation patches in both the northern and southern outer arms are also near corotation, presumably the result of a large scale gravitational collapse of the corotating gas. The main dust lanes for the inner spirals are inside of corotation, and generally on the inside edges of the arms, but the dust at or outside of corotation is very patchy, and, in the north, is on the outside part of the arm. All of these dust positions make sense if the gas shocks while rotating faster than the pattern inside corotation, and slower outside.

The spiral outside of the gap at $0.52R_{25}$ is presumably a material pattern that is driven by the companion (Toomre and Toomre 1972; Tully 1974b). If the rotation curve in Tully (1974a) is extrapolated to $1.0R_{25} = 6.27 \text{ kpc}$, using $\alpha = -0.16$, then the rotation speed there is $22 \text{ km s}^{-1} \text{ kpc}^{-1}$, which is one-fourth the pattern speed of the inner spiral. The inner Lindblad resonance for this rotation speed is at $0.41R_{25} = 2.57 \text{ kpc}$ (for an $\alpha = -0.16$ rotation curve), which is also the position of corotation of the inner spiral (Fig. 10). Thus, the outer spiral may stimulate a response in the vicinity of its inner Lindblad resonance, as illustrated by Howard and Byrd (1989), and this response may stimulate the corotation zone of an inner spiral wavemode, which then causes most of the bright inner spiral structure. Another example of nonlinear mode coupling was discussed by Tagger *et al.* (1987).

The connection between the outer and inner spirals in M51 is not perfectly smooth. Figure 6 reveals a sudden increase in the phase angle of the $m = 2$ spiral component at a radius of $0.5R_{25}$. Neither M81 nor M100 have such increases, and in M51, it occurs at the radius where the outer and inner spirals are proposed to join. Such a jump in phase is consistent with the proposal that the outer and inner spirals are two separate features with different pattern speeds. At the moment, they are not in perfect alignment.

In summary, we have found prominent intensity modulations in the spiral arms of three grand design galaxies, and proposed that some of the minima of these modulations correspond to 4:1 resonances. With the resulting pattern speeds, we then found significant and predictable structures at all of the other resonances, such as sharp terminations of the arms at the outer Lindblad resonances, small inner ovals or circles at the inner Lindblad resonances, prominent wave reflections outside the inner Lindblad resonances in M81 and M100, with weak gaseous extensions of the spirals between these reflection points and the inner resonances, spurs at the 4:1 resonances, located 90° from where the main arms cross the resonance radii, sharp ends to the main dust lanes and star formation ridges at the corotation radii in M100 and M51, prominent interarm star formation at corotation in M100, and a transition in the dust lane position from inside the arms to outside the arms when corotation is crossed in M51.

We also found a remarkable resonance between the outer material spiral arm in M51, triggered by the companion, and an inner spiral wave mode, in the sense that the average position of the inner Lindblad resonances of points along the outer material arm is located at the same position as the corotation resonance of the inner arm. Presumably the stellar response to the outer arms, which is expected at its inner Lindblad resonance (Howard and Byrd 1989), stimulates the inner mode at its most sensitive point, its corotation resonance. This presumably accounts for the unusually strong spiral structure in M51.

Coincidentally, the outer arm pattern speed is approximately one-fourth of the inner pattern speed, suggesting other resonant phenomena as well.

We note that the sequence of galaxies M81, M100, and M51 is a sequence of increasing spiral arm strength and increasing gas abundance. It may be significant that the prominence of the gap at the 4:1 resonance decreases along this sequence, as if the gravitational force from the gas helps to bridge the gap, which, theoretically, is confined to the stars. Also, the prominence of features at the corotation resonance, such as an end to the dust lanes and star formation ridges and the occurrence of prominent interarm star formation, increases along the sequence, as expected for gas-related phenomena.

If our identification of the outer Lindblad resonances with the outer optical edges of the main spirals in M81, M100, and M51 is a general feature of grand design galaxies, then the pattern speeds and all of the resonance locations could, in principle, be determined for any such galaxy, even if the spiral arm gaps at the 4:1 resonance are too faint to observe.

Helpful comments by Drs. G. Contopoulos and C. C. Lin, and the assistance of Miss Kelly V. Beck in preparing Figure 5, are gratefully acknowledged. The plate scanning and image processing were done at IBM with the generous assistance of Drs. J. Angilello, W. Krakow, A. Mobarak, R. Rieker, A. Segmuller, and A. Stein.

REFERENCES

- Angilello, J., Chiang, W. H., Elmegreen, D. M., and Segmuller, A. 1984, in *Proc. Conf. Goddard Astronomical Microdensitometer*, ed. D. A. Klinglesmith (NASA CP-, No. 2317), p. 229.
- Bertin, G., Lin, C. C., Lowe, S. A., and Thurstans, R. P. 1989, *Ap. J.*, **338**, p. 78.
- Contopoulos, G., and Grosbøl, P. 1986, *Astr. Ap.*, **155**, 11.
- . 1988, *Astr. Ap.*, **197**, 83.
- de Vaucouleurs, G., de Vaucouleurs, A., and Corwin, H. G., Jr. 1976, *Second Reference Catalogue of Galaxies* (Austin: University of Texas).
- . 1988, *Astr. Ap.*, **197**, 83.
- Elmegreen, D. M. 1981, *Ap. J. Suppl.*, **47**, 229.
- Grosbøl, P. 1988, *Applied Mathematics, Fluid Mechanics, and Astrophysics: A Symposium to Honor C. C. Lin*, ed. D. Benney, F. Shu, and C. Yuan (Singapore: World Scientific), p. 345.
- Howard, S., and Byrd, G. G. 1989, *A.J.*, submitted.
- Iye, M., Okamura, S., Hamabe, M., and Watanabe, M. 1982, *Ap. J.*, **256**, 103.
- Kaufman, M., Bash, F. N., Hine, B., Rots, A. H., Elmegreen, D. M., Kennicutt, R. C., Jr., and Hodge, P. W. 1989, *Ap. J.*, submitted.
- Kennicutt, R. C., Jr. 1981, *A.J.*, **86**, 1847.
- Lau, Y. Y., Lin, C. C., and Mark, W. K., 1976, *Proc. Nat. Acad. Sci. USA*, **73**, 1379.
- Lin, C. C. 1983, in *Internal Kinematics and Dynamics of Galaxies*, ed. E. Athanassoula (Dordrecht: Reidel), p. 117.
- Rubin, V. C., Ford, W. K., Jr., and Thonnard, N. 1980, *Ap. J.*, **238**, 471.
- Sandage, A. 1961, *Carnegie Institute of Washington Publ. No. 618, Hubble Atlas of Galaxies*.
- Seiden, P. E., Elmegreen, D. M., and Elmegreen, B. G. 1989, in *Le Monde des Galaxies*, ed. F. Bash and M. Capaccioli (Austin: University of Texas), in press.
- Shu, F. N., Milione, V., and Robert, W. W. 1973, *Ap. J.*, **183**, 819.
- Tagger, M., Sygnet, J. F., Athanassoula, E., and Pellat, R. 1987, *Ap. J. (Letters)*, **318**, L43.
- Toomre, A., and Toomre, J. 1972, *Ap. J.*, **178**, 623.
- Tully, R. B. 1974a, *Ap. J. Suppl.*, **27**, 437.
- . 1974b, *Ap. J. Suppl.*, **27**, 449.
- Visser, H. C. D. 1980, *Astr. Ap.*, **88**, 149.

BRUCE G. ELMEGREEN and PHILIP E. SEIDEN: IBM Research Division, T. J. Watson Research Center, P.O. Box 218, Yorktown Heights, NY 10598

DEBRA M. ELMEGREEN: Vassar College Observatory, Poughkeepsie, NY 12601